Solution Conformation of *Eco*RI Restriction Endonuclease Changes upon Binding of Cognate DNA and Mg^{2+} Cofactor†

Heather Watrob,‡ Wei Liu,§ Yu Chen,|| Sue G. Bartlett,§ Linda Jen-Jacobson,⊥ and Mary D. Barkley*,‡

Departments of Chemistry and Biochemistry, Louisiana State University, Baton Rouge, Louisiana 70803, Department of Chemistry, Case Western Reserve University, Cleveland, Ohio 44106, and Department of Biological Sciences, University of Pittsburgh, Pittsburgh, Pennsylvania 15260

Received August 31, 2000; Revised Manuscript Received November 9, 2000

ABSTRACT: *Eco*RI endonuclease has two tryptophans at positions 104 and 246 on the protein surface. A single tryptophan mutant containing Trp246 and a single cysteine labeling site at the N-terminus was used to determine the position of the N-terminus in the protein structure. The N-termini of *Eco*RI endonuclease are essential for tight binding and catalysis yet are not resolved in any of the crystal structures. Resonance energy transfer was used to measure the distance from Trp246 donor to IAEDANS or MIANS acceptors at Cys3. The distance is 36 Å in apoenzyme, decreasing to 26 Å in the DNA complex. Molecular modeling suggests that the N-termini are located at the dimer interface formed by the loops comprising residues 221−232. Protein conformational changes upon binding of cognate DNA and cofactor Mg^{2+} were monitored by tryptophan fluorescence of the single tryptophan mutant and wild-type endonuclease. The fluorescence decay of Trp246 is a triple exponential with lifetimes of 7, 3.5, and 0.7 ns. The decay-associated spectra of the 7- and 3.5-ns components have emission maxima at ∼345 and ∼338 nm in apoenzyme, which shift to ∼340 and ∼348 nm in the DNA complex. The fluorescence quantum yield of the single tryptophan mutant drops 30% in the DNA complex, as compared to 10% for wild-type endonuclease. Fluorescence changes of Trp104 upon binding of DNA were inferred by comparison of the decay-associated spectra of wild type and single tryptophan mutant. Fluorescence changes are related to changes in proximity and orientation of quenching functional groups in the tryptophan microenvironments, as seen in the crystal structures.

Like other Type II restriction endonucleases,[1] *Eco*RI is a homodimer that cleaves its palindromic recognition sequence GAATTC in the presence of cofactor Mg^{2+} (*2*). *Eco*RI endonuclease finds its recognition site on a large DNA by facilitated diffusion (*3*−*5*), whereby the protein binds nonspecifically to DNA (*6*, *7*) and diffuses along the DNA helix to its specific site (*8*). Like other highly specific DNA binding proteins, the structural and energetic complementarity of the protein−DNA interface of the specific complex is achieved in a cooperative, concerted manner via major conformational transitions, in which both the structures of the apoenzyme and the DNA site are dramatically changed (*9*−*11*); 1QC9.pdb (*12*). The conformational transitions are accompanied by burial of large amounts of previously hydrated nonpolar surface and restriction in configurational and vibrational degrees of freedom of protein, DNA, and water molecules trapped at the protein−DNA interface (*13*−*15*). These factors are absent in nonspecific complexes (*14*).

Protein conformational changes associated with specific DNA binding are apparent in the crystal structures of the apoproteins and cognate DNA complexes for *Eco*RV (*16*−*18*), *Bam*HI (*19*, *20*), and *Eco*RI (*10*, *21*), 1QC9.pdb. Recently, seven crystal structures of *Eco*RI apoenzyme and cognate DNA complexes were determined by John M. Rosenberg and co-workers (1QC9.pdb, 1ERI.pdb, 1CKQ.pdb, 1QPS.pdb, 1CL8.pdb, 1QRH.pdb, 1QRI.pdb). The protein conformational change in the *Eco*RI−DNA complex includes local folding of residues 122−129 in the inner arm and retraction of N-terminal residues 17−19 and C-terminal residues 276−277. The N-terminal residues 2−16 are not resolved in any of the *Eco*RI structures.[2] This unresolved region is essential for DNA cleavage as well as maximal stability of the complex (*22*). Proteolytic deletion of the first 11 residues completely abolished cleavage activity, yet the

† This work was supported by NIH Grants GM29207 and GM35009.

* To whom correspondence should be addressed at Department of Chemistry, Case Western Reserve University, 10900 Euclid Avenue, Cleveland, OH 44106. E-mail: mdb4@po.cwru.edu.

‡ Case Western Reserve University.

§ Louisiana State University.

|| Current address: BD Pharmingen, 10975 Torreyana Road, San Diego, CA 92121.

⊥ University of Pittsburgh.

[1] Abbreviations: Bis-tris propane, 1,3-bis[tris(hydroxymethyl)-methylamino]propane; DAS, decay-associated spectrum; DTT, dithiothreitol; EDTA, ethylenediaminetetraacetic acid; 1,5-IAEDANS, *N*-iodoacetyl-*N*′-(5-sulfo-1-naphthyl)ethylenediamine; IAEDANS-Cys, conjugate of 1,5-IAEDANS and *N*-acetyl Cys; IAEDANS-N3CW104Y, conjugate of 1,5-IAEDANS and N3CW104Y mutein; MIANS, 2-(4′-maleimidylanilino)naphthalene-6-sulfonic acid; MIANS-Cys, conjugate of MIANS and *N*-acetyl Cys; MIANS-N3CW104Y, conjugate of MIANS and N3CW104Y mutein; RMSD, root-mean-square deviation; SDS−PAGE, sodium dodecyl sulfate polyacrylamide gel electrophoresis; Tricine, *N*-[tris-(hydroxymethyl)-methyl]-glycine; Tris, tris-(hydroxymethyl)-amino methane.

[2] Amino acid residues in *Eco*RI endonuclease are numbered according to the gene sequence. Residue 1 (fMet) is missing in mature enzyme (*1*).

10.1021/bi002055j CCC: $20.00
Published on Web 12/23/2000

truncated enzyme still bound specifically to cognate DNA with about a factor of 60 lower binding affinity. Removal of the first three residues had little effect, only lowering binding affinity by a factor of 2. This suggests a key role for the N-terminal region of *Eco*RI in the conformational transitions leading to tight DNA binding and catalysis.

Previously, we showed by site-directed fluorescence spectroscopy (*23*) and chemical cross-linking that the N-termini of *Eco*RI are close together on the protein surface, presumably at the dimer interface (*24*). Neither cognate DNA nor cofactor Mg^{2+} affected the proximity and mobility of the second amino acid residue in the protein sequence. *Eco*RI endonuclease has two tryptophans at positions 104 and 246, which are on the protein surface remote from the protein−DNA interface (*10*, *21*). This paper examines the effects of cognate DNA and Mg^{2+} on the tryptophan environments in a single tryptophan mutant and wild-type enzyme. In addition, the distance between Trp246 and the N-termini is determined by resonance energy transfer in the absence and presence of DNA and Mg^{2+}. The energy transfer data together with the crystal structures specify the location of the N-termini.

EXPERIMENTAL PROCEDURES

Materials. *N*-iodoacetyl-*N*′-(5-sulfo-1-naphthyl)ethylenediamine was from Molecular Probes (Eugene, OR) and 2-(4′-maleimidylanilino)naphthalene-6-sulfonic acid was from Sigma Chemical Co. (St. Louis, MO). Glass-distilled glycerol (EM Science, Cherry Hill, NJ) was used in buffers for optical experiments. The 13-nt sequence d(TCGCGAATTCGCG) was synthesized by Gene Lab in the Louisiana State University School of Veterinary Medicine or by the Pittsburgh DNA Synthesis Facility, purified, and annealed (*24*). All other chemicals were the highest grade available.

NaCl buffer contains 10 mM sodium phosphate buffer, pH 7.0, NaCl at the indicated concentration, 1 mM EDTA, and 7 mM β-mercaptoethanol. The following NaCl buffers, 10% glycerol without β-mercaptoethanol, were used for optical experiments: endonuclease and *N*-acetylcysteine conjugates, 0.6 M NaCl; *Eco*RI−DNA complex, 0.1 M NaCl; *Eco*RI−Mg^{2+} complex, 0.6 M NaCl, 20 mM $MgCl_2$.

Site-Directed Mutagenesis. Site-directed mutagenesis was performed using the ALTERED SITES system from Promega (Madison, WI). Asn3Cys mutation was described previously (*24*). The gene fragment between *Hind*III and *Sal*I sites for residues 68−277 of the C-terminal sequence of *Eco*RI endonuclease and methyltransferase from an expression vector pSCC2 (*25*) was cloned into pSELECT-1 vector in the multiple cloning site. Mutagenesis was conducted using the double-stranded template protocol provided by the manufacturer. The oligonucleotide carrying the Trp104Tyr mutation, d(GGC TTC AGC AAC AAG TAC TAC TCT ATA TTC ACC ATA ATC ATC), also carried a silent mutation to create a diagnostic *Sca*I restriction site (AGTACT) for screening mutants. The *Hind*III−*Sal*I insert carrying the newly created *Sca*I restriction site in pSELECT-1 was cloned back into the modified pSCC2 expression vector (*24*), which was then renamed pW104Y referring to the Trp104Tyr mutation. DNA sequencing of the insert confirmed the mutation. The *Mlu*I−*Hind*III gene fragment in pW104Y was replaced with the *Mlu*I−*Hind*III fragment from pN3C carrying the Asn3Cys mutation to give the expression vector pN3CW104Y carrying the double mutation Asn3Cys and Trp104Tyr.

Protein Purification. Wild-type and mutant endonucleases were purified and assayed as described elsewhere (*24*). N3CW104Y mutein eluted at the same salt concentration as wild-type enzyme on the three columns used: P-11 phosphocellulose, HTP hydroxyapatite, and BioRex-70 (*26*). The enzymes were >99% pure as judged by SDS−PAGE. Protein concentration was determined by the BioRad protein assay using an *Eco*RI endonuclease standard solution, whose concentration had been determined by amino acid analysis. Molarity of endonuclease solutions is based on a dimer molecular mass of 62 kDa. Purified endonuclease was stored at −70 °C in 0.6 M NaCl buffer, 10% glycerol.

Equilibrium association constants K_A for endonuclease and 24-nt cognate DNA d(GGGCGGGTGCGAATTCGCGGGCGG) were determined by membrane filtration as described previously (*24*). Binding conditions were 10 mM Bis-tris propane, pH 7.3, 0.16 M NaCl, 1 mM EDTA, 5 μM DTT, and 100 μg/mL bovine serum albumin, 22 °C.

Fluorescent Labeling. Labeling of N3C and N3CW104Y muteins with 1,5-IAEDANS or MIANS was performed as before (*24*). The labeling reaction for 1,5-IAEDANS was allowed to go for 10 h. Because MIANS is essentially nonfluorescent until reacted with sulfhydryl, the MIANS reaction was followed by fluorescence at 320 nm excitation wavelength, 450 nm emission wavelength. The reaction with MIANS was complete after 15 min for [MIANS]/[N3CW104Y] ratios of 0.6−6.4. Ratios of 2.4 and 6.4 gave the same intensity increment, consistent with accessibility of Cys3 and inaccessibility of Cys218 (*24*). The extent of labeling after removal of unreacted probe was estimated spectrophotometrically, using extinction coefficients of 6.1×10^3 M^{-1} cm^{-1} at 337 nm for 1,5-IAEDANS and 1.7×10^4 M^{-1} cm^{-1} at 327 nm for MIANS (*27*). With two cysteines per homodimer, labeling was stoichiometric with molar ratios of probe to endonuclease between 1.96 and 2.0.

The labeling site was confirmed by peptide mapping. Enzyme was digested by partial acid hydrolysis in 60% formic acid for 3 days at 37 °C (*28*). Peptides were separated by RP-HPLC (C_{18} column, 300 Å pore size, 5 μm particle size), gradient: 35−55% B in 25 min; A, 0.1% TFA in water; B, 0.085% TFA in acetonitrile/2-propanol (1:1). Peptides were detected by UV (214 nm) and fluorescence (tryptophan, excitation 280 nm, emission 350 nm; IAEDANS, excitation 330 nm, emission 480 nm; MIANS, excitation 320 nm, emission 430 nm). Formic acid cleaves *Eco*RI endonuclease at the unique Asp74−Pro75 bond to generate 8.2 kDa N-terminal and 22.9 kDa C-terminal fragments. Peptides were identified in a separate experiment with unlabeled enzyme by monitoring tryptophan fluorescence of the 22.9 kDa C-terminal fragment during HPLC and by high-resolution SDS−PAGE using a Tris/Tricine buffer system (*29*). IAEDANS or MIANS fluorescence was observed only in the N-terminal fragment of labeled enzyme, indicating specific labeling of Cys3 and no reaction of Cys218. Labeled enzyme was stored at −70 °C in 0.6 M NaCl buffer, 10% glycerol, and was dialyzed into the same buffer without β-mercaptoethanol prior to optical experiments.

N-Acetylcysteine conjugates were made by reacting 1,5-IAEDANS and MIANS with a 5-fold molar excess of

N-acetylcysteine at room temperature in the dark for 24 h. The product was purified by flash chromatography on a silica column. Purified conjugate migrated as a single spot on TLC developed with *n*-butanol/water/acetic acid (2:2:1).

Fluorescence Measurements. Absorption and fluorescence measurements were performed at 4 °C as described (*24*). Excitation wavelength was 295 nm for tryptophan and 320 nm for 1,5-IAEDANS and MIANS. Fluorescence quantum yields Φ were measured relative to tryptophan in water using a value of 0.14 at 25 °C (*30*). Time-correlated single photon counting measurements used a rhodamine 6G dye laser for tryptophan and a DCM dye laser for 1,5-IAEDANS and MIANS. Decay data were collected in 1024 channels of 12−83 ps/channel. Temperature was maintained at 4 °C by a circulating water bath. Sample compartment was purged with nitrogen to prevent condensation. Decay curves were deconvolved using the Beechem global program (*31*). Goodness of fit was judged by reduced chi square χ_r^2 and the autocorrelation function of the weighted residuals.

Fluorescence intensity decays $I(t)$ were fit to a sum of exponentials

$$I(t) = \sum \alpha_i \exp(-t/\tau_i) \quad (1)$$

with amplitudes α_i and lifetimes τ_i. Decay curves acquired at different emission wavelengths were deconvolved simultaneously assuming that lifetimes but not amplitudes were independent of wavelength. Some data sets had <1% of a 10−50 ps component due to scattered light. Decay-associated emission spectra $F_i(\lambda)$ were calculated by combining the steady-state emission spectrum $F(\lambda)$ and time-resolved data.

$$F_i(\lambda) = \alpha_i(\lambda)\tau_i F(\lambda)/\sum \alpha_i(\lambda)\tau_i \quad (2)$$

In constructing the DAS for wild type, the steady-state emission spectrum was peak normalized. The steady-state spectra of wild type in the presence of DNA and Mg^{2+} were scaled relative to apoenzyme based on protein absorbance at 295 nm. Assuming equal extinction coefficients for Trp104 and Trp246, wild type has about twice the extinction coefficient of the single tryptophan mutant. In constructing the DAS for N3CW104Y mutein, the steady-state emission spectra in the absence and presence of DNA and Mg^{2+} were scaled to the same protein concentration as wild-type based on protein absorbance at 295 nm. Figure 1 shows that the relative intensities of the scaled spectra correlate well with relative quantum yields.

Fluorescence anisotropy decays $r(t)$ were fit to a sum of exponentials

$$r(t) = \sum \beta_i \exp(-t/\phi_i) \quad (3)$$

with preexponential β_i and rotational correlation time ϕ_i. The initial anisotropy $r(0) = \Sigma\beta_i$. Individual polarized decays $I_{VV}(t)$ and $I_{VH}(t)$ are deconvolved simultaneously with a magic angle decay $I(t)$

$$I_{VV}(t) = I(t)[1 + 2r(t)]/3 \quad (4a)$$

$$I_{VH}(t) = GI(t)[1 - r(t)]/3 \quad (4b)$$

where the correction factor $G \approx 1$ in our instrument.

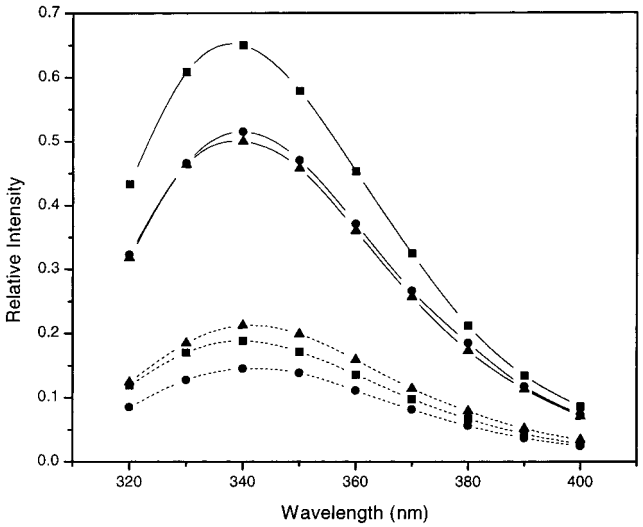

FIGURE 1: Steady-state emission spectra normalized to wild-type *Eco*RI endonuclease apoenzyme as described in Experimental Procedures. (—) wild type: (■) apoenzyme, (●) *Eco*RI−DNA complex, (▲) *Eco*RI−Mg^{2+} complex. (···) N3CW104Y mutein: (■) apoenzyme, (●) N3CW104Y-DNA complex, (▲) N3CW104Y−Mg^{2+} complex.

Fluorescence Energy Transfer. For a unique distance r between donor and acceptor, the efficiency of energy transfer E is

$$E = 1 - \tau_{DA}/\tau_D \quad (5)$$

where τ_D and τ_{DA} are the donor lifetimes in the absence and presence of acceptor. Average lifetimes $\bar{\tau}$ of multiexponential donor decays were used in eq 5.

$$\bar{\tau} = \sum \alpha_i\tau_i/\sum \alpha_i \quad (6)$$

In the presence of two acceptors, τ_{DA} becomes

$$\tau_{DA} = \tau_D + k_{T1} + k_{T2} \quad (7)$$

where k_{Ti} is the rate of energy transfer from the donor to acceptor i,

$$k_{Ti} = \tau_D^{-1}(R_{0i}/r_i)^6 \quad (8)$$

so that E becomes

$$E = [(R_{01}/r_1)^6 + (R_{02}/r_2)^6]/\{1 + [(R_{01}/r_1)^6 + (R_{02}/r_2)^6]\} \quad (9)$$

where R_{0i} is the Förster critical distance for transfer from donor to acceptor i. The R_0 value in Å for a donor/acceptor pair was determined from

$$R_0 = 0.211(n^{-4}\Phi_D\kappa^2 J)^{1/6} \quad (10)$$

where n is the refractive index of the medium taken to be 1.4, Φ_D is the donor quantum yield in the absence of acceptor, κ^2 is the orientation factor, and J is the spectral overlap integral in M^{-1} cm^{-1} nm^4. The overlap integral was calculated from the donor emission spectrum $F_D(\lambda)$ and acceptor absorption spectrum $\epsilon_A(\lambda)$. For random orientation

$$J = \int F_D(\lambda)\epsilon_A(\lambda)\lambda^4 d\lambda / \int F_D(\lambda)d\lambda \quad (11)$$

Table 1: Fluorescence Quantum Yields and Emission Maxima

sample	Φ^a	λ_{max} nm	$\bar{\tau}^b$ ns
W246 in N3CW104Y[c]	0.18	338	5.1
+DNA	0.13	338	4.2
$+Mg^{2+}$	0.19	340	4.3
W246 + W104 in wild type[c]	0.24	337	4.5
+DNA	0.22	338	4.6
$+Mg^{2+}$	0.21	339	3.9
IAEDANS-Cys[d]		492	
IAEDANS-N3CW104Y[d]		485	
MIANS-Cys[d]		459	
MIANS-N3CW104Y[d]		450	

[a] Errors are ± 0.02. [b] Emission wavelength 350 nm. [c] Excitation wavelength 295 nm. [d] Excitation wavelength 320 nm.

of donor emission and acceptor absorption dipoles, the value of $\kappa^2 = 2/3$; the corresponding values of R_0 and r are designated $R_0(2/3)$ and $r_{2/3}$. The maximum uncertainty in distance due to an unknown value of κ^2 was estimated from steady-state and time-resolved anisotropy data by the method of Dale et al. (*32*) as described in Lakowicz et al. (*33*). Maximum κ^2_{max} and minimum κ^2_{min} values calculated from depolarization factors were used to calculate r_{max} and r_{min} values.

Molecular Modeling. Molecular modeling was performed using InsightII 97.0 from Molecular Simulations Inc. (San Diego, CA) on a Silicon Graphics Indy workstation. Superposition was performed by best fit of the C_α carbons using Swiss PdbViewer (*34*) on a Macintosh G3. The following structures were downloaded from the Protein Data Bank (*12*). 1QC9.pdb is a 3.0 Å structure of wild-type *Eco*RI endonuclease. 1ERI.pdb is a 2.7 Å structure, and 1CKQ.pdb is a 1.85 Å structure of wild-type complexed with 13-mer cognate DNA. 1QPS.pdb is a 2.5 Å structure of wild-type complexed with Mn^{2+} and 13-mer cognate DNA cleaved at the recognition sequence. 1CL8.pdb is a 1.8 Å structure of wild-type complexed with 13-mer DNA duplex with the inner adenine in the recognition sequence replaced by purine. 1QRH.pdb is a 2.5 Å structure of active site mutant R145K complexed with 13-mer cognate DNA. 1QRI.pdb is a 2.6 Å structure of active site mutant E144D complexed with 13-mer cognate DNA. The structures were superimposed to a best fit of the C_α carbons using the 1.85 Å *Eco*RI−DNA complex (1CKQ.pdb) as reference structure.

RESULTS

Single Tryptophan Mutant. Substitution of Trp104 with tyrosine does not affect the activity of *Eco*RI endonuclease. N3CW104Y mutein, which has a single tryptophan at position 246, cleaves λ-DNA into the same restriction fragments as wild type as judged by agarose gel electrophoresis. The mutein binds to cognate 24 bp oligomer with the same affinity ($7.6 \pm 0.2 \times 10^{10}$ M^{-1}) as wild type ($7.5 \pm 0.3 \times 10^{10}$ M^{-1}). The absorption maximum at 278 nm is the same in the single tryptophan mutant and wild-type enzyme. The fluorescence emission maxima at 338 nm are also the same within error (Table 1), consistent with partially exposed tryptophans. Binding of cognate DNA or cofactor Mg^{2+} does not shift the spectra of either the single tryptophan mutant or wild-type enzyme. The fluorescence quantum yield of Trp246 is 0.18 (Table 1). DNA binding quenches the fluorescence of Trp246 about 30%, whereas Mg^{2+} binding has no effect within error. The quenching of Trp246 fluorescence by cognate DNA indicates a conformational change near the protein surface far from the DNA binding site.

Changes in protein conformation reported by Trp246 were explored in more detail by time-resolved fluorescence studies of N3CW104Y mutein. Time-resolved emission spectral data of N3CW104Y in the absence and presence of cognate DNA or Mg^{2+} were acquired at 10-nm intervals from 320 to 400 nm. In all cases, global analysis gave good fits to three exponentials with lifetimes of about 7, 3.5, and 0.7 ns. Fits to four exponentials resolved a stray light component of <50 ps with some improvement in χ_r^2. Table 2 gives the results from the four-exponential fits omitting the stray light component. The average lifetime of Trp246 drops about 15% in both the DNA and Mg^{2+} complexes. The drops in quantum yield and average lifetime upon binding of DNA or Mg^{2+} are about the same within error. These drops result primarily from changes in the relative amplitudes of the different lifetime components. The lifetimes do not appear to change appreciably in the presence of DNA or Mg^{2+} cofactor. This hypothesis was put to a more rigorous test by global analyses of the wavelength data sets for N3CW104Y mutein, N3CW104Y−DNA complex, and N3CW104Y−Mg^{2+} complex with one to three of the lifetimes linked. Global analyses of any two data sets with all lifetimes linked gave acceptable χ_r^2 values. However, a comprehensive global analysis of the three data sets with all lifetimes linked gave a poor fit. A series of analyses linking various lifetimes confirmed no significant lifetime changes upon binding of Mg^{2+} and a slight increase in the long lifetime from 6.7 to 7.2 ns upon binding of DNA.

Figures 2 and 3 show the decay-associated emission spectra of the 7- and 3.5-ns lifetime components of Trp246 in N3CW104Y mutein. (The poorly resolved 0.7-ns DAS is not shown.) The 7- and 3.5-ns DAS have maxima at 345 and 338 nm. The 7-ns DAS of Trp246 is quenched upon addition of DNA. A >5 nm blue shift accompanies this intensity drop, indicating a change in tryptophan environment. The 3.5-ns DAS is only slightly quenched by DNA but red shifted by >10 nm. Mg^{2+} binding has much smaller effects, causing only slight enhancement of both DAS with no spectral shift for the 7-ns DAS and <5-nm red shift for the 3.5-ns DAS.

Time-resolved emission anisotropy of N3CW104Y mutein was measured in the absence and presence of cognate DNA or Mg^{2+} to examine the mobility of Trp246. Fits of the anisotropy data to a single exponential gave acceptable χ_r^2 values, which were slightly improved by assuming two rotational correlation times (Table 3). The 1-ns rotational correlation time was attributed to internal motion of Trp246, and the 100-ns rotational correlation time was attributed to protein global motion. The rotational correlation time of *Eco*RI endonuclease estimated by the Stokes−Einstein equation is about 73 ns (*24*). The initial anisotropy $r(0) = 0.14$ of Trp246 is low as compared to the fundamental anisotropy of 0.25 for tryptophan in water (*35*) and 0.21−0.26 for tryptophan in rigid proteins (*36*−*39*) at 295 nm excitation wavelength, diagnostic of fast motion unresolved on the 25-ns time scale of the experiment. The amplitude of the ~100-ns rotational correlation time increases from 0.11 for N3CW104Y mutein to 0.13 for N3CW104Y−Mg^{2+}

Table 2: Tryptophan Fluorescence Decay Parameters[a]

sample	$\alpha_1(350)$[b]	τ_1 ns	$\alpha_2(350)$[b]	τ_2 ns	τ_3 ns	$\bar{\tau}(350)$ ns	χ_r^2
W246 in N3CW104Y[c]	0.57	6.7	0.35	3.4	0.69	5.1	1.37
+DNA	0.37	7.2	0.39	3.4	0.70	4.2	1.46
$+Mg^{2+}$	0.42	6.8	0.38	3.5	0.71	4.3	1.43
W246 in IAEDANS-N3CW104Y[d]	0.46 ± 0.02	6.57 ± 0.06	0.43 ± 0.03	3.67 ± 0.05	0.57 ± 0.02	4.7	0.97
+DNA	0.35 ± 0.01	5.0 ± 0.1	0.35 ± 0.01	1.92 ± 0.08	0.22 ± 0.01	2.5	1.23
$+Mg^{2+}$	0.46 ± 0.01	5.90 ± 0.06	0.34 ± 0.01	2.5 ± 0.1	0.50 ± 0.05	3.7	1.09
W246 in MIANS-N3CW104Y[d]	0.56 ± 0.02	6.06 ± 0.06	0.29 ± 0.02	2.44 ± 0.09	0.22 ± 0.01	4.1	1.17
+DNA	0.27 ± 0.05	5.3 ± 0.1	0.33 ± 0.03	1.9 ± 0.2	0.26 ± 0.06	2.2	1.41
$+Mg^{2+}$	0.42 ± 0.05	6.1 ± 0.2	0.37 ± 0.03	2.8 ± 0.3	0.63 ± 0.09	3.7	1.06
W246 + W104 in wild type[c]	0.25	7.1	0.66	4.1	0.95	4.6	1.29
+DNA	0.45	6.3	0.54	3.2	0.63	4.6	2.38
$+Mg^{2+}$	0.20	7.2	0.60	3.8	0.65	3.9	1.72

[a] Excitation wavelength 295 nm. [b] $\Sigma\alpha_i(350) = 1$. [c] Global analysis of data from 320−400 nm emission wavelength, 10 nm intervals. [d] Errors are standard deviations of at least three experiments at 350 nm emission wavelength.

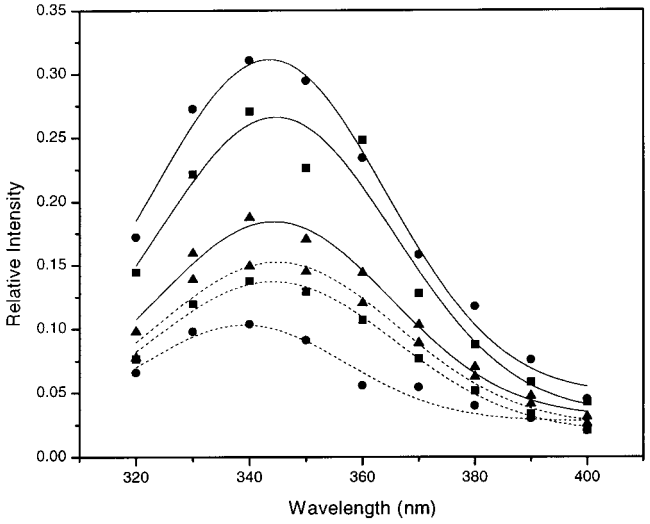

FIGURE 2: Decay-associated emission spectra of 7-ns component normalized to steady-state spectra in Figure 1. (—) wild type: (■) apoenzyme, (●) *Eco*RI−DNA complex, (▲) *Eco*RI−Mg^{2+} complex; (···) N3CW104Y mutein: (■) apoenzyme, (●) N3CW104Y−DNA complex, (▲) N3CW104Y−Mg^{2+} complex.

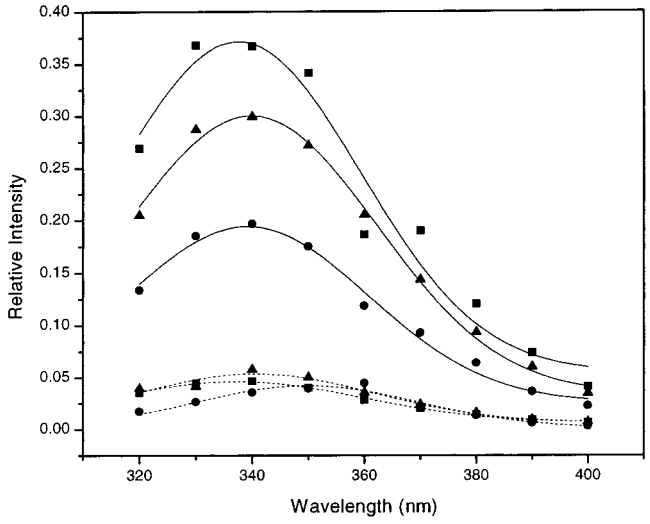

FIGURE 3: Decay-associated emission spectra of 3.5- or 4-ns component normalized to steady-state spectra in Figure 1. (—) wild type: (■) apoenzyme, (●) *Eco*RI−DNA complex, (▲) *Eco*RI−Mg^{2+} complex; (···) N3CW104Y mutein: (■) apoenzyme, (●) N3CW104Y−DNA complex, (▲) N3CW104Y−Mg^{2+} complex.

complex and to 0.17 for N3CW104Y-DNA complex, suggesting partial hindrance of the fast motion of Trp246 in the complexes.

Wild-Type Endonuclease. Wild-type enzyme contains two tryptophans per subunit, which together have a quantum yield of 0.24 (Table 1). The net effect of DNA or Mg^{2+} on wild-type fluorescence is about 10% quenching, in agreement with previous observations of *Eco*RI−DNA complex (*40*, *41*). This becomes more interesting in light of the fluorescence changes in the single tryptophan mutant. The wild-type tryptophans are too far apart for Trp−Trp energy transfer, because $R_0 = 4-16$ Å for self-transfer (*42*) and the closest distance between Trp104 and Trp246 in any of the crystal structures is the intrasubunit distance of ∼30 Å. Therefore, the contributions of Trp104 and Trp246 to wild type fluorescence are essentially independent. The steady-emission spectra in Figure 1 show that the two tryptophans do not contribute equally to wild-type fluorescence. W104 appears to dominate the spectra. This is not surprising, as the two tryptophans are in unique environments (Figure 4).

Time-resolved measurements in the absence and presence of cognate DNA and Mg^{2+} give lifetimes of 6−7, 3−4, and 0.6−1 ns, similar to the values for Trp246, with χ_r^2 values of 1.3−2.4 (Table 2). The higher χ_r^2 values reflect greater lifetime heterogeneity in the DNA and Mg^{2+} complexes. Linking only one or two lifetimes reduces χ_r^2 to 1.3. The average lifetime and quantum yield change little if at all within error upon binding of DNA or Mg^{2+}. The lifetimes of the 7- and 4-ns components decrease somewhat in the *Eco*RI−DNA complex. However, there is no change in average lifetime because of compensating changes in amplitudes. Binding of Mg^{2+} causes only small decreases in the amplitudes of the 7- and 4-ns components.

The decay-associated spectral changes upon binding of DNA differ in the single tryptophan mutant and wild-type enzyme. The 7-ns DAS of wild type is slightly enhanced with little shift in maximum. Since the 7-ns DAS of Trp246 is quenched upon addition of DNA, the enhancement in wild type must be due to an increase in intensity of the 7-ns DAS of Trp104. Conversely, the 4-ns DAS of wild type is significantly quenched by DNA without a spectral shift. Recall that Trp246 had only a slight decrease in intensity but a significant spectral shift. This is strong evidence that the large decrease in the 4-ns DAS of wild type is due to Trp104. Unlike the mutein, wild type exhibits a significant decrease in the 7-ns DAS upon binding of Mg^{2+}. This must

Table 3: Anisotropy Decay Parameters[a]

sample	β_1	ϕ_1 ns	β_2	ϕ_2 ns	$r(0)$	χ_r^2
W246 in N3CW104Y[b]	0.119 ± 0.007	53 ± 6			0.119 ± 0.007	1.55
	0.035 ± 0.001	0.90 ± 0.06	0.108 ± 0.007	103 ± 6	0.143 ± 0.008	1.20
+DNA	0.14 ± 0.04	120 ± 30			0.14 ± 0.04	1.74
	0.033 ± 0.003	0.51 ± 0.01	0.17 ± 0.01	172 ± 4	0.20 ± 0.01	1.64
+Mg^{2+}	0.14 ± 0.02	80 ± 40			0.14 ± 0.02	1.67
	0.032 ± 0.005	0.6 ± 0.3	0.13 ± 0.03	100 ± 20	0.16 ± 0.03	1.38
IAEDANS-Cys[c,d]	0.215 ± 0.003	0.33 ± 0.05			0.214[e]	1.87
IAEDANS-N3C[c,f]	0.09	1.7	0.11	149	0.20	1.73
MIANS-Cys[g,h]	0.333 ± 0.002	0.85 ± 0.05			0.364[e]	1.42
MIANS-N3C[g,i]	0.02	0.65	0.29	160	0.31	1.70

[a] Errors are standard deviations of at least three experiments. [b] Excitation wavelength 295 nm, emission wavelength 350 nm. [c] Excitation wavelength 320 nm, emission wavelength 500 nm. [d] $\bar{\tau}$= 14.4 ns. [e] Fundamental anisotropy r_0 values from ref *45*. [f] $\bar{\tau}$= 14.1 ns. [g] Excitation wavelength 320 nm, emission wavelength 450 nm. [h] $\bar{\tau}$= 0.35 ns. [i] $\bar{\tau}$= 3.4 ns.

be due to Trp104, as the 7-ns DAS of Trp246 increases slightly in the presence of Mg^{2+}. The 4-ns DAS of wild type decreases slightly with addition of Mg^{2+} and shifts <5 nm to the red.

Labeled Muteins. The labeled N3CW104Y muteins bind tightly to DNA with K_A values lower by factors of 2−3 than unlabeled mutein: $4.5 \pm 0.2 \times 10^{10}$ M^{-1} for IAEDANS−N3CW104Y and $2.7 \pm 0.3 \times 10^{10}$ M^{-1} for MIANS−N3CW104Y. The fluorescence emission spectra of probes in the protein conjugates are blue-shifted 7−9 nm as compared to the cysteine conjugates (Table 1). The fluorescence of 1,5-IAEDANS and MIANS is environmentally sensitive (*43*, *44*). The blue shift indicates that these probes are in a more hydrophobic environment on labeled N3CW-104Y mutein relative to aqueous solution.

Fluorescence anisotropy decays were measured for labeled N3C muteins. The anisotropy decays of IAEDANS- and MIANS-N3C were best fit by two exponentials (Table 3). As before, the short rotational correlation time represents local motion of the probe and the long rotational correlation time represents overall tumbling of the protein. Comparison of the $r(0)$ values of labeled muteins and the fundamental anisotropies r_0 of the cysteine conjugates reveals some unresolved fast motion in the observed anisotropy decay of MIANS-N3C, but not IAEDANS-N3C. On the basis of the relative β_i values, the fraction of probe undergoing rapid internal motion is about 50% for IAEDANS and 20% for MIANS. These results support our previous conclusion from studies of pyrene-labeled N3C mutein that the N-termini are on the protein surface (*24*).

Energy Transfer. The average lifetime of Trp246 decreased from 5.1 ns in N3CW104Y mutein to 4.7 ns in the IAEDANS conjugate and 4.1 ns in the MIANS conjugate (Table 2). Energy transfer efficiencies were calculated from eq 5. The labeled N3CW104Y mutein has two Trp246 donors and two labeled Cys3 acceptors per homodimer. As discussed above, energy transfer between the two Trp246 residues is negligible. Only one of the tryptophans will be excited per homodimer. However, the excited Trp246 has two possible acceptors: a labeled Cys3 in its own subunit and a labeled Cys3 in the other subunit. These two Cys3 residues are close together at the dimer interface in the absence and presence of cognate DNA and cofactor Mg^{2+}, as judged by excimer formation and covalent cross-linking (*24*). Therefore, we assume that the intra- and intersubunit distances between Trp246 and the two labeled Cys3 acceptors are roughly the same. If we further assume the same R_0 value for transfer from Trp246 to each labeled Cys3, then eq 9 simplifies considerably

$$E = 2R_0^6/[r^6 + 2R_0^6] \quad (12)$$

and the distance r between Trp246 donor and labeled Cys3 acceptor is given by

$$r = R_0[2(1/E - 1)]^{1/6} \quad (13)$$

Use of a single R_0 is valid, because R_0 depends only on the Trp246 quantum yield in the absence of acceptor, the overlap of the Trp246 emission and probe absorption spectra, and the relative orientation of the two chromophores. The first two are identical for both inter- and intrasubunit pairs, and the third should be similar if not identical, because the anisotropy data indicate some mobility of both donor and acceptor (Table 3).

Distances calculated from eq 13 are given in Table 4. Both probes gave very similar distances: 37 Å for IAEDANS and 35 Å for MIANS assuming $\kappa^2 = 2/3$. Binding of cognate DNA decreased these distances to 25 and 27 Å, respectively. Binding of cofactor Mg^{2+} had smaller effects on the distance. Upper and lower limits for the orientation factor κ^2 were calculated using the time-resolved anisotropy data in Table 3 and literature values for the fundamental anisotropies (*33*, *45*). The corresponding values of r_{max} and r_{min} were estimated from the κ_{max}^2 and κ_{min}^2 values (Table 4). The distance range averaged about 16 Å. Since both indole (*42*) and dansyl (*43*) fluorophores have mixed polarizations, the actual range of distances should be even narrower (*46*).

DISCUSSION

Tryptophan is widely used as an intrinsic fluorescence probe of protein conformational changes upon ligand binding. The fluorescence lifetime and intensity are sensitive to the local environment of the indole ring. In addition, energy transfer from a tryptophan donor to a fluorescent label provides distance information. A single tryptophan mutant of *Eco*RI homodimer with a specific labeling site at the N-terminus allowed us to monitor local structural changes around Trp246 upon cognate DNA or cofactor Mg^{2+} binding and to locate the N-termini on the protein surface. This N3CW104Y mutein has the same DNA binding and cleavage properties as wild-type enzyme. Labeling Cys3 with IAEDANS or MIANS decreased the binding affinity only

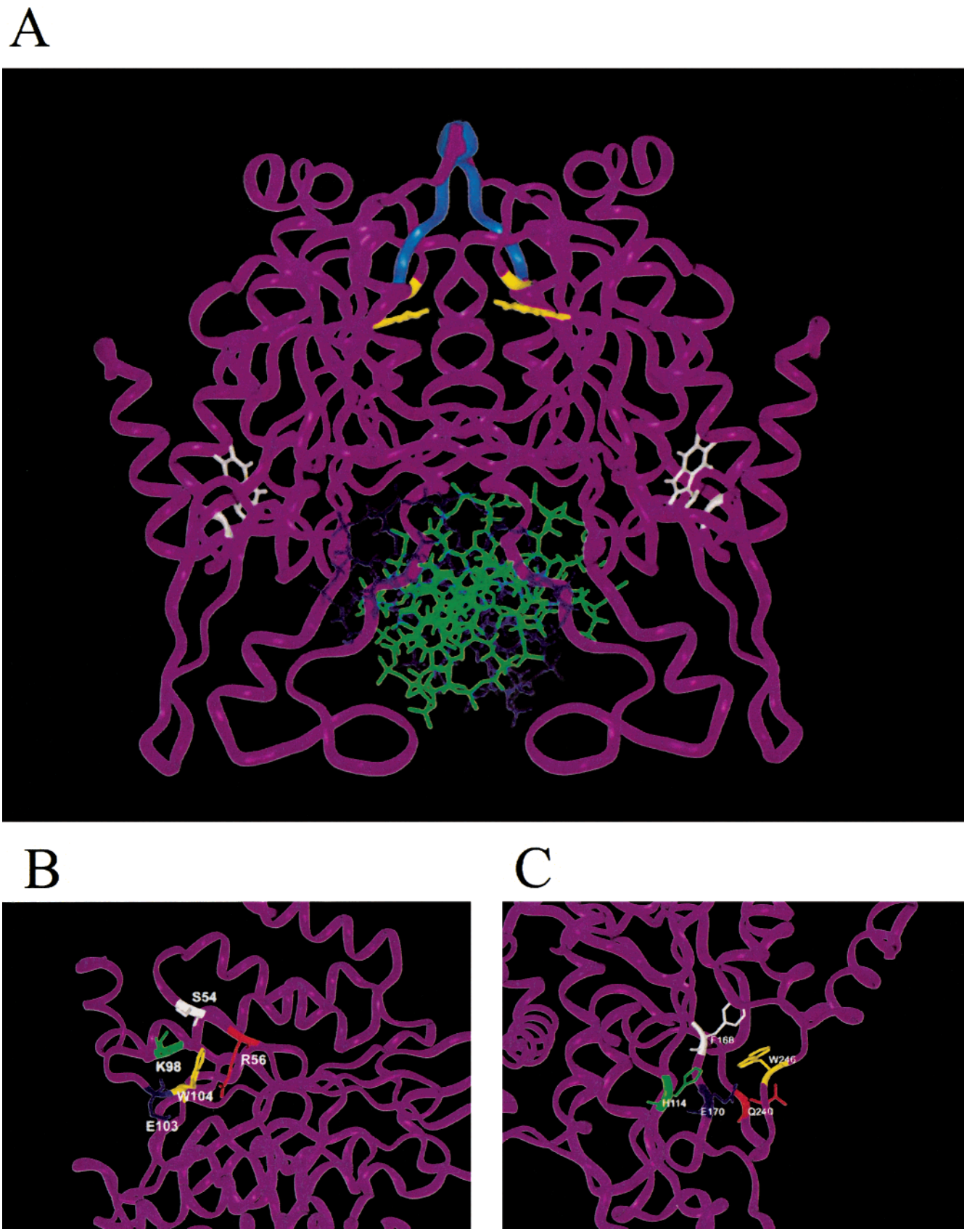

FIGURE 4: *Eco*RI−DNA complex (1CKQ.pdb). (A) *Eco*RI homodimer depicting (green and dark blue) cognate DNA, (yellow) Trp104, (white) Trp246, and (light blue) proposed location of N-termini at intersecting loops. (B) Microenvironment of (yellow) Trp104 and nearby side chains: (white) S54, (red) R56, (green) K98, (dark blue) E103. (C) Microenvironment of (yellow) Trp246 and nearby side chains: (green) H114, (white) F168, (dark blue) E170, (red) Q240.

0.3 or 0.6 kcal/mol. Thus, we expect results of fluorescence studies of labeled muteins to apply to wild-type enzyme.

Location of N-Termini. The distance between Trp246 and fluorescent probes at Cys3 in *Eco*RI homodimer was

Table 4: Fluorescence Energy Transfer

sample	E	$R_0(2/3)^a$ (Å)	κ_{max}^2	κ_{min}^2	$r_{2/3}$ (Å)	r_{max} (Å)	r_{min} (Å)
IAEDANS-N3CW104Y[b]	0.08	21.7	2.52	0.20	36.6	45.7	29.9
+DNA	0.40	20.5	3.02	0.14	24.6	31.7	19.0
$+Mg^{2+}$	0.14	21.8	2.72	0.18	33.1	41.9	26.6
MIANS-N3CW104Y[c]	0.20	24.7	2.75	0.15	34.9	44.2	27.2
+DNA	0.48	23.4	3.31	0.09	26.6	34.8	19.1
$+Mg^{2+}$	0.14	24.9	2.97	0.12	37.8	48.5	28.4

[a] R_0 was calculated for $\kappa^2 = 2/3$. [b] $J = 5.63 \times 10^{13}$ M^{-1} cm^{-1} nm^4. [c] $J = 1.23 \times 10^{13}$ M^{-1} cm^{-1} nm^4.

estimated via resonance energy transfer. Both IAEDANS and MIANS gave similar distances of ~36 Å in apoenzyme (Table 4). Binding of cognate DNA decreased this distance by about 10 Å for both probes. Binding of cofactor Mg^{2+} probably has negligible effects. We can interpret the apparent distance change upon DNA binding in three ways: (i) the distance r between labeled Cys3 and Trp246 decreased, (ii) the relative orientation of the two chromophores changed, or (iii) a combination of (i) and (ii). Previously, we showed that the N-termini of N3C mutein are close together and partially immobilized on the protein surface (*24*). Formation of a disulfide bond between the two Cys3s and of excimers between pyrene-labeled Cys3s limits the distance between N-termini to 2.5−18 Å in both the presence and absence of DNA. We do not expect the W104Y mutation to have a significant effect on the distance between N-termini, as it does not alter enzyme activity. The distance r between Trp246 and labeled Cys3 measured by energy transfer depends on the relative orientation of the chromophore transition dipoles through κ^2. In the labeled muteins, the anisotropy data show that both chromophores undergo local and segmental motions (Table 3), which tend to randomize their orientations. The anisotropy data were used to calculate maximum and minimum values for κ^2, which dictates a ±8 Å uncertainty in the measured r values (Table 4). Given the range of distances between the N-termini and the calculated range in r values due to uncertainties in κ^2, we cannot distinguish interpretations (i) and (ii).

Figure 4, panel A, of the DNA complex shows the first α-helix α1 at the outside of each subunit. Both α1 helices are pointing away from the DNA interface and in the direction of the loops formed by residues 221−232. The tips of the α1 helices turn back toward the protein. In the apoenzyme structure, α-helix α1 also points away from the DNA and toward the loops, but the tips turn outward away from the protein. Superposition of the structure of wild-type apoenzyme (1QC9.pdb) upon the highest resolution structure of *Eco*RI−DNA complex (1CKQ.pdb) gave a RMSD value of ~0.7 Å. The intersubunit distance between the first resolved residue of the N-terminus (Ser17) decreases by > 10 Å in the DNA complex (81.1 Å for apoenzyme vs 68.5 Å for DNA complex). Visual inspection suggests that the N-termini are slightly frayed in different directions in the two structures. We propose that this results from a change in conformation of the unresolved region of the N-termini, as other intra- and intersubunit distances are the same in apoenzyme and DNA complex. A change in backbone trajectory of Ser17, Gln18, and Gly19 at the tip of α1 might translate to a change in distance or orientation of the N-termini relative to Trp246.

The crystal structure of *Eco*RI−DNA complex (1CKQ.pdb) limits the possible locations of the N-termini at the dimer interface. Given the symmetry and experimental distance constraints, the most likely location is the vicinity of the intersecting loops formed by residues 221−232. Looking down the DNA helix, these two loops span the central plane of the complex that runs through the subunit interface and lie on the opposite side of the structure from the DNA binding interface (Figure 4, panel A). The loops cross each other at residues 227−232 to form part of the subunit interface. The residues closest to their counterparts in the other subunit are Ser229 and Ile230, with intersubunit distances of 5.9 and 4.6 Å. Assuming that the N-terminal region traverses the protein surface, the shortest distance from Ser17 to these residues is about 42−47 Å. A fully extended polypeptide chain of 15 amino acids has a length of 54 Å, more than enough to cover this distance. The energy transfer experiments give through-space distances between Trp246 and the two fluorescent probes at Cys3 of about 36 Å in apoenzyme and 26 Å in the DNA complex. Intrasubunit through-space distances between Trp246 and Ser229 and Ile 230 from the crystal structures are 37 and 35 Å in apoenzyme and 38 and 35 Å in the DNA complex. Intersubunit distances are 39 and 36 Å in apoenzyme and DNA complex. The energy transfer distance of 36 Å measured for apoenzyme is consistent with the proposed location of the N-termini near Ser229 and Ile230.

Local Conformational Changes. Typical of single tryptophan containing proteins, the single tryptophan at position 246 in N3CW104Y mutein gave triple exponential fluorescence decays. The origin of this complexity is unknown. However, the decay-associated emission spectra clearly reveal conformational changes in the microenvironment of Trp246. The intensity changes and spectral shifts of the 7- and 3.5-ns DAS upon binding cognate DNA are most likely attributable to global conformational changes in the protein that affect the microenvironment of Trp246. Figure 4, panel C, shows the microenvironment of Trp246 in the wild type *Eco*RI−DNA complex (1CKQ.pdb). Trp246 is partially buried in the loop region just before the last α-helix α6 at the C-terminus of each subunit about 15 Å from the DNA duplex (Figure 4, panel A). His114, Glu170, and Gln240 are the closest amino acid side chains likely to affect tryptophan fluorescence. All three side chains quench 3-methylindole fluorescence by an excited-state electron transfer mechanism in intermolecular quenching experiments: the imidazole ring of histidine is a strong quencher, protonated carboxyl is a moderate quencher, and the amide group of glutamine is a weak quencher. In the crystal structure of apoenzyme (1QC9.pdb), the partially accessible imidazole ring of His114 is about 8.9 Å away from the indole ring, the buried carboxyl of Glu170 is 6.5 Å away, and the amide group of Gln240 is about 4.1 Å away. The peptide bond has been shown to quench indole fluorescence via intramolecular electron transfer (*47*). The peptide bonds of Phe168, Leu169, Tyr238, Thr239, Glu245, and Trp246 are within 6 Å of the indole ring. Superposition of the structures of apoenzyme and DNA complex shows relatively little change in overall peptide backbone structure but clear changes in position and orientation of the side chain functional groups. Distances from the indole ring to four of the six nearby peptide bonds decrease slightly in the DNA complex. The distance to the

imidazole ring of His114 decreases slightly to 8.5 Å accompanied by a distinctive change in orientation, and the distance of the amide group of Gln240 increases dramatically to 6.0 Å.

Clearly, Trp104 dominates the fluorescence of wild type. This suggests greater static quenching of Trp246 than Trp104 fluorescence in wild type. Conformational changes in the microenvironment of Trp104 are readily apparent by comparing the decay-associated emission spectra of the two tryptophans in wild type with the single tryptophan in N3CW104Y. Trp104 is more solvent-accessible than Trp246 in both crystal structures as judged by Connolly surface analysis. It is located at the N-terminal end of β3, which is within the β-meander formed by antiparallel β-sheets β1, β2, and β3 (*21*). Trp104 is sandwiched between four hydrophilic residues Ser54, Arg56, Lys98, and Glu103 (Figure 4, panel B) and is located ~25 Å from the DNA (Figure 4, panel A). The only possible quenching side chain is the positively charged amino group of Lys98, which is 6.0 Å from the indole ring in the apoenzyme. Lys quenches by an excited-state proton-transfer mechanism (*48*). The solvent-exposed carboxyl of Glu103 is most likely deprotonated and thus unable to quench tryptophan fluorescence. The peptide bonds within 6 Å of the indole ring of Trp104 are Val97, Gly102, Glu103, and Trp104. Comparison of the structures of apoenzyme and DNA complex reveals a small decrease in distance of the Lys98 amino group to 5.8 Å in the DNA complex. As in the case of Trp246, relatively little change was observed in the peptide backbone in the vicinity of Trp104 when the two structures were superimposed. Slight increases in distance between the indole ring and the peptide bonds of Trp104 and Glu103 are offset by decreases in distance of Val97 and Gly102. The presence of fewer quenching functional groups in the microenvironment of Trp104 appears to account for the reduced static quenching.

The N-terminal regions of *Eco*RI endonuclease spanning from Ser17−Ser2 of one subunit to Ser2−Ser17 of the other subunit can be regarded as a long-open loop (*49*). Loops are typically found on the protein surface and play important roles in biological function (*50*). In the case of *Eco*RI endonuclease, the hydrophilic N-terminal region lies on the protein surface (*24*), stabilizes the *Eco*RI−DNA complex, and is essential for DNA cleavage (*22*). The tryptophan residues of *Eco*RI endonuclease are embedded in the protein surface, some distance from both subunit and DNA interfaces. The alteration in tryptophan microenvironment upon DNA binding implies structural perturbations at the protein surface. Conformational changes at the protein−DNA interface are thus transmitted to the protein surface. Presumably, interactions of the N-terminal region with the protein surface would likewise be felt at the protein−DNA interface.

ACKNOWLEDGMENT

We thank Dr. Jay R. Knutson for helpful discussions about decay-associated spectra.

REFERENCES

1. Rubin, R. A., Modrich, P., and Vanaman, T. C. (1981) *J. Biol. Chem. 256*, 2140−2142.
2. Pingoud, A., and Jeltsch, A. (1997) *Eur. J. Biochem. 246*, 1−22.
3. Jack, W. E., Terry, B. J., and Modrich, P. (1982) *Proc. Natl. Acad. Sci. U.S.A. 79*, 4010−4014.
4. Enbrecht, H.-J., Pingoud, A., Urbanke, C., Maass, G., and Gualerzi, C. (1985) *J. Biol. Chem. 260*, 6160−6166.
5. Terry, B. J., Jack, W. E., and Modrich, P. (1985) *J. Biol. Chem. 260*, 13130−13137.
6. Langowski, J., Pingoud, A., Goppelt, M., and Maass, G. (1980) *Nucleic Acids Res. 8*, 4727−4736.
7. Terry, B. J., Jack, W. E., Rubin, R. A., and Modrich, P. (1983) *J. Biol. Chem. 258*, 9820−9825.
8. Wright, D. J., Jack, W. E., and Modrich, P. (1999) *J. Biol. Chem. 274*, 31896−31902.
9. McClarin, J. A., Frederick, C. A., Wang, B.-C., Greene, P., Boyer, H. W., Grable, J., and Rosenberg, J. M. (1986) *Science 234*, 1526−1541.
10. Kim, Y., Grable, J. C., Love, R., Greene, P. J., and Rosenberg, J. M. (1990) *Science 249*, 1307−1309.
11. Lesser, D. R., Kurpiewski, M. R., and Jen-Jacobson, L. (1990) *Science 250*, 776−786.
12. Berman, H. M., Wetbrook, J., Feng, Z., Gilliland, G., Bhat, T. N., Weissig, H., Shindyalov, I. N., and Bourne, P. E. (2000) *Nucleic Acids Res. 28*, 235−242.
13. Ha, J.-H., Spolar, R. S., and Record, M. T., Jr. (1989) *J. Mol. Biol. 209*, 801−816.
14. Jen-Jacobson, L., Engler, L. E., Amers, J. T., Kurpiewski, M. R., and Grigorescu, A. (2000) *Supramol. Chem. 12*, 143−160.
15. Cao, D., and Jen-Jacobson, L., unpublished results.
16. Winkler, F. K., Banner, D. W., Oefner, C., Tsernoglu, D., Brown, R. S., Heathman, S. P., Bryan, R. K., Martin, P. D., Petratos, K., and Wilson, K. S. (1993) *EMBO J. 12*, 1781−1795.
17. Vipond, I. B., and Halford, S. E. (1993) *Mol. Microbiol. 9*, 225−231.
18. Kostrewa, D., and Winkler, F. K. (1995) *Biochemistry 34*, 683−696.
19. Newman, M., Strzelecka, T., Dorner, L. F., Schildkraut, I., and Aggarwal, A. K. (1994) *Nature 368*, 660−664.
20. Newman, M., Strzelecka, T., Dorner, L., Schildkraut, I., and Aggarwal, A. (1995) *Science 269*, 656−663.
21. Rosenberg, J. M. (1991) *Curr. Opin. Struct. Biol. 1*, 104−113.
22. Jen-Jacobson, L., Lesser, D., and Kurpiewski, M. (1986) *Cell 45*, 619−629.
23. Ujwal, M. L., Jung, H., Bibi, E., Manoil, C., Altenbach, C., Hubbell, W. L., and Kaback, H. R. (1995) *Biochemistry 34*, 14909−14917.
24. Liu, W., Chen, Y., Watrob, H., Bartlett, S. G., Jen-Jacobson, L., and Barkley, M. D. (1998) *Biochemistry 37*, 15457−15465.
25. Cheng, S.-C., Kim, R., King, K., Kim, S.-H., and Modrich, P. (1984) *J. Biol. Chem. 259*, 11571−11575.
26. Greene, P. J., Heyneker, H. L., Boliver, F., Rodriguez, R. L., Beltach, M. C., Covarrubias, A. A., Backman, K., Russel, D. J., Tait, R., and Boyer, H. W. (1978) *Nucleic Acids Res. 5*, 2373−2380.
27. Haugland, R. P. (1996) *Handbook of Fluorescent Probes and Research Chemicals*, 6th ed., Molecular Probes, Inc., Eugene, OR.
28. Landon, M. (1977) *Methods Enzymol. 47*, 145−149.
29. Schagger, H., and von Jagow, G. (1987) *Anal. Biochem. 166*, 368−379.
30. Chen, R. F. (1967) *Anal. Lett. 1*, 35−42.
31. Beechem, J. M. (1989) *Chem. Phys. Lipids 50*, 237−251.
32. Dale, R. E., Eisinger, J., and Blumberg, W. E. (1979) *Biophys. J. 26*, 161−194.
33. Lakowicz, J. R., Gryczynski, I., Chueng, H. C., Wang, C.-K., Johnson, M. L., and Joshi, N. (1988) *Biochemistry 27*, 9149−9160.
34. Guex, N., and Peitsch, M. C. (1997) *Electrophoresis 18*, 2714−2723. http://www.expasy.ch/spdbv/
35. Shen, X., and Knutson, J. R. (2000) *J. Am. Chem. Soc.* submitted for publication.
36. Ross, J. B. A., Schmidt, C. J., and Brand, L. (1981) *Biochemistry 20*, 4369−4377.

37. Chen, L. X.-Q., Longworth, J. W., and Fleming, G. R. (1987) *Biophys. J. 51*, 865−873.
38. Kim, S.-J., Lewis, M. S., Knutson, J. R., Porter, D. K., Kumar, A., and Wilson, S. H. (1994) *J. Mol. Biol. 244*, 224−235.
39. Tcherkasskaya, O., Pitsyn, O. B., and Knutson, J. R. (2000) *Biochemistry 39*, 1879−1889.
40. Jhon, N.-I., Casas-Finet, J. R., Maki, A. H., and Modrich, P. (1988) *Biochim. Biophys. Acta 949*, 189−194.
41. Alves, J., Urbanke, C., Fliess, A., Maass, G., and Pingoud, A. (1989) *Biochemistry 28*, 2879−2888.
42. Lakowicz, J. R. (1999) *Principles of Fluorescence Spectroscopy*, 2nd ed., Kluwer Academic/Plenum Publishers, New York.
43. Hudson, E. N., and Weber, G. (1973) *Biochemistry 12*, 4154−4161.
44. Gupte, S. S., and Lane, L. K. (1979) *J. Biol. Chem. 254*, 10361−10367.
45. Xing, J., and Cheung, H. (1995) *Biochemistry 34*, 6475−6487.
46. Haas, E., Katchalski-Katzir, E., and Steinberg, I. Z. (1978) *Biochemistry 17*, 5064−5070.
47. Chen, Y., Liu, B., Yu, H.-T., and Barkley, M. D. (1996) *J. Am. Chem. Soc. 118*, 9271−9278.
48. Chen, Y., and Barkley, M. D. (1998) *Biochemistry 37*, 9976−9982.
49. Martin, A. C. R., Toda, K., Stirk, H. J., and Thornton, J. M. (1995) *Protein Eng. 8*, 1093−1101.
50. Leszczynski, J. F., and Rose, G. D. (1986) *Science 234*, 849−855.

BI002055J